DESIGN OF TRANSFER LINE CLAMPS

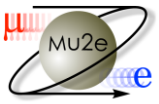

Mu2e Experiment

Final Report Summer Student 2015

Fermilab

Eleonora Bargiacchi

Supervisor: Richard Schmitt; Co-Supervisor: Nandhini Dhanaraj

Table of contents

1. Introduction

The transfer lines which run between the feedboxes and the magnets house all the piping for the cooling of the magnets. The bus bar which runs from the magnet and terminates into the power leads are housed in the TL as well. The bus bars will be cooled by clamping the cooling tube and the conductors. The cooling is affected by the insulation around the conductors and also the thermal contact resistance between the different interfaces, factors which are determinant in our operating conditions (in vacuum and at cryogenic temperatures). The goal of the task is to design a clamp proposing an appropriate insulation scheme and test it.

1.1. Mu2e Experiment

Mu2e experiment purposes to design and build a facility that will enable the most sensitive search ever made for the coherent conversion of muons into electrons in the field of an atomic nucleus.

The theory that lies behind the physics of the experiment won't be discussed in this paper. We will focalize our attention on the structure of the experiment and zoom in the components that are significant for our analysis.

Mu2e experiment is made up of three solenoids that have to operate as a single, integrated magnetic system: the Production Solenoid (PS), the Transport Solenoid (TS) – divided into upstream and downstream sections - and the Detector Solenoid. Their main function is to generate magnetic fields to efficiently collect and transport muons from the production target to the muon stopping target while minimizing the transmission of other particles. Electrons are transported from the stopping target to detector elements where a uniform and precisely measured magnetic field is used to measure the momentum of electrons.

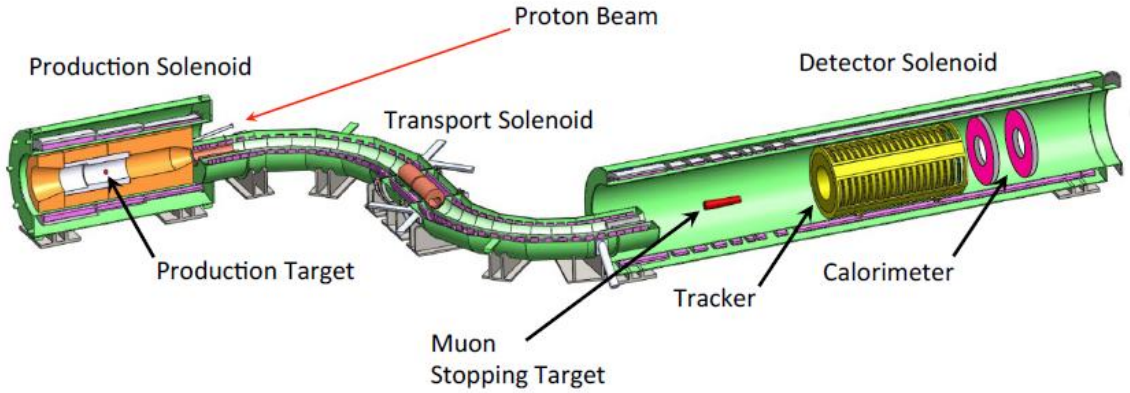

FIGURE 1. THE MU2E DETECTOR

Additional infrastructure is essential to run the solenoids; this includes power supply systems, quenching protection, cooling system, control and safety systems, mechanical supports.

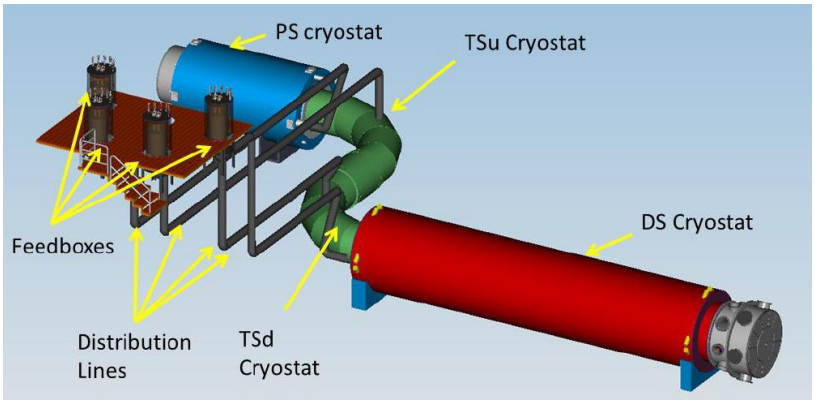

FIGURE 2. MU2E SUPERCONDUCTING SOLENOID SYSTEM

1.1.1. Cryogenic System

In order to maintain NbTi superconductivity and avoid quenching, the whole complex needs to be cooled down. Each part has different temperature requirements, depending on the local intensity of magnetic field (for instance, maximum allowable temperature is 5.10 K when operating at 4.6 T peak axial field and 4.85 K when operating at 5.0 T peak axial field). As far as transfer line is concerned, a precise temperature requirement hasn't been set yet, provided the temperature is lower than 6 K. A temperature margin of 1.5 K has been established to allow a safe run out of the magnets in any operating conditions.

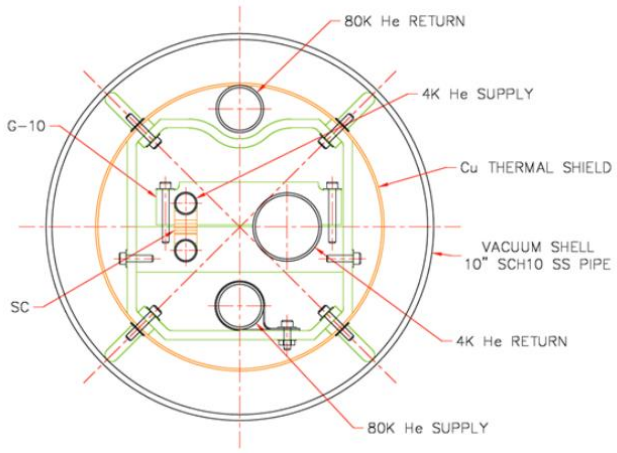

FIGURE 3. CROSS SECTION OF CRYOGENIC DISTRIBUTION LINE

Cooling system is divided into four semi-autonomous cryogenic units, each supplying one solenoid. Coils will be properly insulated and cooled indirectly (by conduction) to a thermosiphon circuit. Refrigerators (feedboxes) located in a separate building will supply 4.70 K liquid helium and 80 K liquid nitrogen for the entire system. The two circuits are divided from each other by a 80K copper thermal shield, and insulated from the environment by a stainless steel vacuum tube. Multilayer insulation (MLI) will be used to shield radiation between 300K and 80K shield and between 80 K circuit and 4.7K circuit. Supports for pipes are G10 plates.

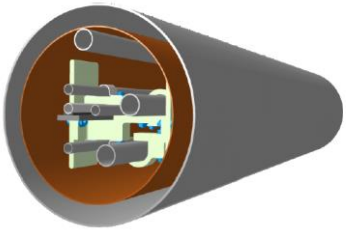

Each line will be approximately 20 m long.

The estimated 80 K radiation heat load hitting the surfaces which face the copper thermal shield is 0.2 W/m.

FIGURE 4. SECTION OF TRANSFER LINE

2. Clamp modeling

2.1. Coil design

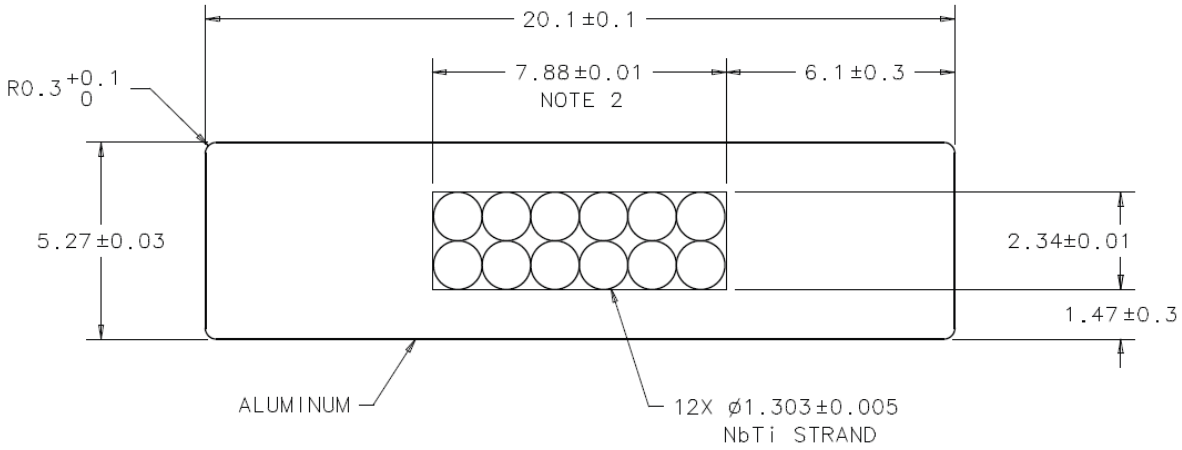

FIGURE 5. CROSS SECTION OF DS1 TRANSFER LINE SUPERCONDUCTOR

The superconductor is copper stabilized Niobium Titanium strand. Copper RRR 80 and NbTi are modeled as two different parts with a cross area ratio of 1:1. The cable is further stabilized with high conductivity Aluminum (Al RRR 800).

2.2. Coil insulation scheme

Insulation plays a fundamental role since, besides providing high electrical strength and resistance to radiation, it must show relatively low thermal resistance to allow a proper cooling of the coils.

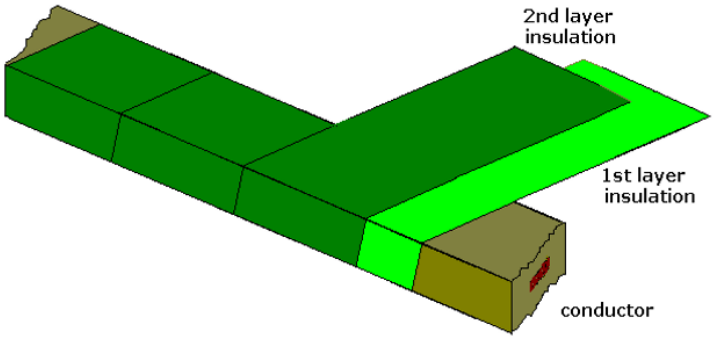

FIGURE 6. TWO LAYER KAPTON INSULATION OF SUPERCONDUCTOR

The nominal cable insulation thickness is 50.8 μm (0.002 inches), made of two layers kapton 25.4 μm each.

Between the clamp and the external kapton, a 1 mm G10 layer is inserted. The two insulated superconductors are kept separated by a 1.5 mm G10 spacer, which insulates the two conductors electrically, preventing them from short circuit.

The complete insulation scheme for the superconductors is shown in figures 8 and 9.

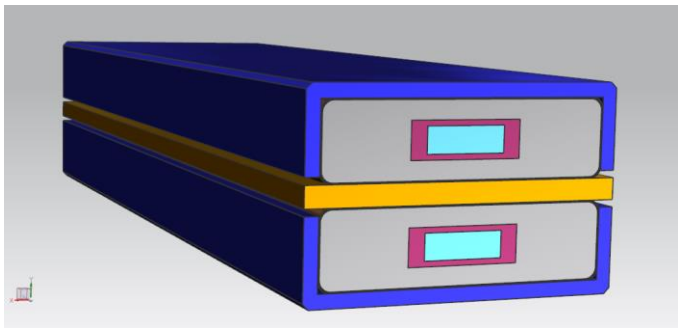

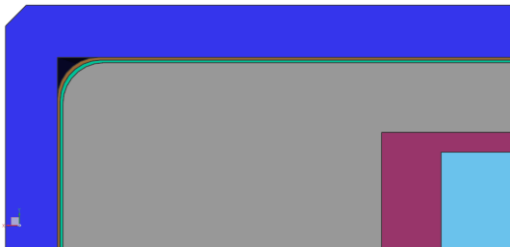

FIGURE 7. DETAIL OF COMPLETE INSULATION SCHEME

FIGURE 8. 3D NX MODEL OF THE COMPLETE INSULATION SCHEME

2.3. Clamp 3D model

3D model of the cooling clamp is shown in picture 9.

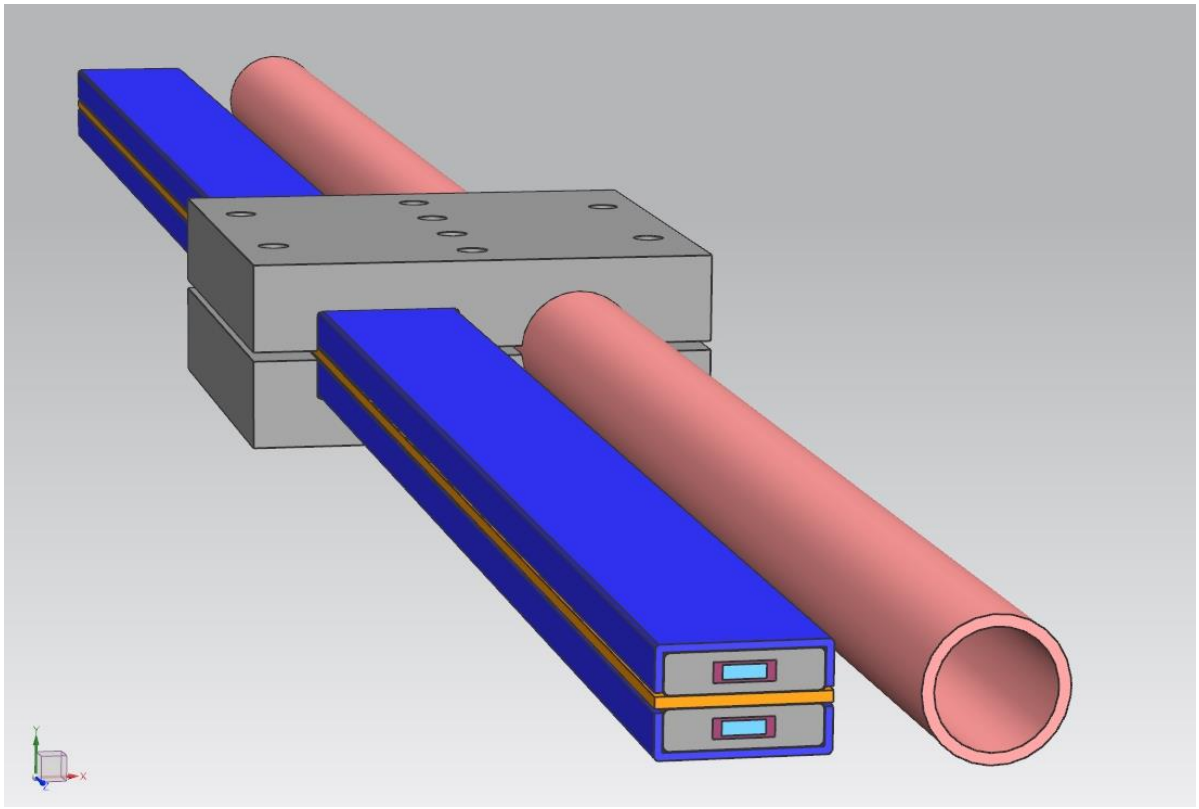

FIGURE 9. 3D NX MODEL OF COOLING CLAMP

The clamp and the 16 mm (0.625") helium pipe are made of Aluminum 6061 T6, a very conductive alloy which exhibits good mechanical properties and good weldability. Bolt number has been chosen by analyzing contact pressure distribution. Their configuration derives from a compromise between having a high contact pressure on the superconductor (which implies a more efficient cooling due to higher contact conductance) and limiting their number to facilitate the assembly.

3. Thermal Contact Conductance (TCC)

The study of thermal contact conductance is of significant importance at cryogenic temperatures. Contact resistance can be a serious problem in cryogenic systems, particularly at ultra-low temperatures where thermal conductivities are low and cooling powers often limited. In most cases, in fact, temperature drop across joints represents the bigger fraction of the total temperature drop. There isn't any unified theory about TCC. An accurate prediction of values of thermal contact conductance under certain conditions is hard, due to the large variety of parameters influencing the phenomenon. Anyway, many efforts have been done to find approximate correlations, most of which have been experimentally verified. The models used for this purpose give approximate values to within an order of magnitude.

3.1. Theory of Thermal Contact Conductance

Heat flux over an interface between two surfaces in contact is subjected to a thermal contact resistance, defined as the ratio between the temperature drop across the interface and the total heat flux over the interface:

$$R_j = \frac{\Delta T}{qA} = \frac{1}{h_j A}$$

The inverse of contact resistance is the joint thermal conductance: $h_j = \frac{1}{R_j A} = \frac{Q}{A\Delta T}$.

It is made up of three contribution: $h_j = h_r + h_g + h_c$.

Radiative conduction (h_r) is due to radiation between the two interfaces. This contribution is significant only at relatively high temperature so, at our operating temperature, we can assume $h_r \approx 0$.

Gap conductance (h_g) is the conduction through the small gas-filled gaps between the two surfaces in contact. In vacuum, $h_g = 0$.

Therefore, in our case, thermal contact conductance can be assumed equal to joint thermal conductance: $h_j = h_c = \frac{Q}{A\Delta T}$.

The main reason for the presence of thermal contact resistance is that the real contact area is less than the apparent one. The entity of this difference is strictly dependent on several parameters of the interfaces in contact, such as surface roughness (or, more in general, the geometry of the contacting solids), surface hardness, thermal conductivity, modulus of elasticity and contact pressure, which this paper will take into account. Other factors eventually influencing thermal contact resistance are: gap thickness, linear coefficient of thermal expansion and thermal interface material.

3.2. Models for Thermal Contact Conductance

Several empirical formulas to calculate thermal contact conductance between two interfaces in contact have been found. Basically, the material can deform in plastic or elastic way. Since we don't know how the materials deform at 4.7 K, TCC is evaluated for both ways of deformation.

3.2.1. Parameters

Since the two surfaces in contact have different geometric properties, TCC values in models are calculated as depending on conventional average parameters, so called effective values, which take into account the properties of the two materials of the joint.

The effective thermal conductivity is defined as: $K_S = \frac{2K_1K_2}{K_1+K_2}$ where k_1 and k_2 are the thermal conductivity of the two materials of the joint.

Surface roughness can be described by two parameters:

- $\sigma_s = \sqrt{(\sigma_1^2 + \sigma_2^2)}$ effective RMS surface roughness (with $\sigma = \sqrt{\frac{1}{L}\int_0^L y^2(x)dx}$).

  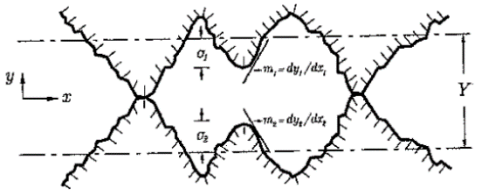

  The parameter which is always available is the arithmetic average of roughness $R_a = \frac{1}{L}\int_0^L |y(x)|dx$, deriving from surface finishing. R_a and σ can be related assuming a Gaussian distribution of asperities: $\sigma = \sqrt{\frac{\pi}{2}}R_a \approx 1.25R_a$
- $m_s = \sqrt{(m_1^2 + m_2^2)}$ effective absolute mean asperity slope

  A large variety of empirical relations have been proposed to express m as a function of roughness in order to limit the amount of variables to measure.
  Lambert and Fletcher [6] and Tanner and Fahoum [7] found out the following correlations between absolute average asperity slope and RMS surface roughness:

$$m = 0.076(\sigma \cdot 10^6)^{0.52}$$
$$m = 0.152(\sigma \cdot 10^6)^{0.4}$$

3.2.2. Elastic Model

Assuming elastic deformation leads to a correlation where TCC is proportional to the inverse of Young modulus: $h_c \propto \frac{k_s m_s}{\sigma_s}(\frac{P}{E'})^{\alpha}$

Mikic (1974) proposed a mathematical model for the deformation and thermal contact conductance of two nominal flat surfaces in contact, in a vacuum environment under condition of negligible radiation.

$$h_c = 1.55\frac{k_s m_s}{\sigma_s}\left(\frac{P\sqrt{2}}{E' m_s}\right)^{0.94} \text{ with } E' = \frac{E_1 E_2}{E_1(1-\nu_2^2)+E_2(1-\nu_1^2)}$$

3.2.3. Plastic Models

Assuming plastic deformation leads to correlations that depends on surface hardness of joint materials. All four different models analyzed below show the same dependence on geometrical parameters, thermal conductivity and pressure: $h_c \propto \frac{k_s m_s}{\sigma_s}\left(\frac{P}{H_c}\right)^{\alpha}$

- Tien, 1968: $h_c = 0.55\frac{k_s m_s}{\sigma_s}\left(\frac{P}{H_C}\right)^{0.85}$
- Cooper, Mikic and Yovanovich, 1969: $h_c = 1.45\frac{k_s m_s}{\sigma_s}\left(\frac{P}{H_C}\right)^{0.985}$
- Mikic, 1974: $h_c = 1.13\frac{k_s m_s}{\sigma_s}\left(\frac{P}{H_C}\right)^{0.94}$
- Yovanovich, 1982: $h_c = 1.25\frac{k_s m_s}{\sigma_s}\left(\frac{P}{H_C}\right)^{0.95}$

3.3. Results

In order to cool the superconductor down, heat flux has to come across five interfaces. Contacts between Nb-Ti and Copper RRR 80 and between Copper RRR 80 and Aluminum RRR 800 are considered bounded since parts of one single extrusion.

TABLE 1. MATERIAL PROPERTIES

	Hardness Hc (MPa)	Thermal conductivity k (W/m*K)	Young Modulus E (GPa)	Poisson's Ratio ν	Ra (μm)	σ (μm)	m (m)
Al 6061-T6	1049	11.2	77.75	0.33	0.8	1.00	0.125
Al RRR 800	147	1690	77	0.33	3.2	4.00	0.219
Kapton	259	0.0119	5.034	0.34	3.2	4.00	0.219
G10	191	0.0611	29.1	0.21	3.2	4.00	0.219

TABLE 2. JOINT PARAMETERS

	k_s (W/m*K)	σ_s (μm)	m_s (m)	E' (MPa)
Al RRR 800 - Kapton	0.024	5.66	0.310	5340.22
Kapton - Kapton	0.012	5.66	0.310	2486.00
Kapton - G10	0.020	5.66	0.310	4795.38
G10 - Al 6061 T6	0.122	4.12	0.253	22568.46

Al 6061 T6 – Al 6061 T6	11.20	1.41	0.177	43628.26

Resulting values of TCC as a function of contact pressure for all five interfaces are shown below.

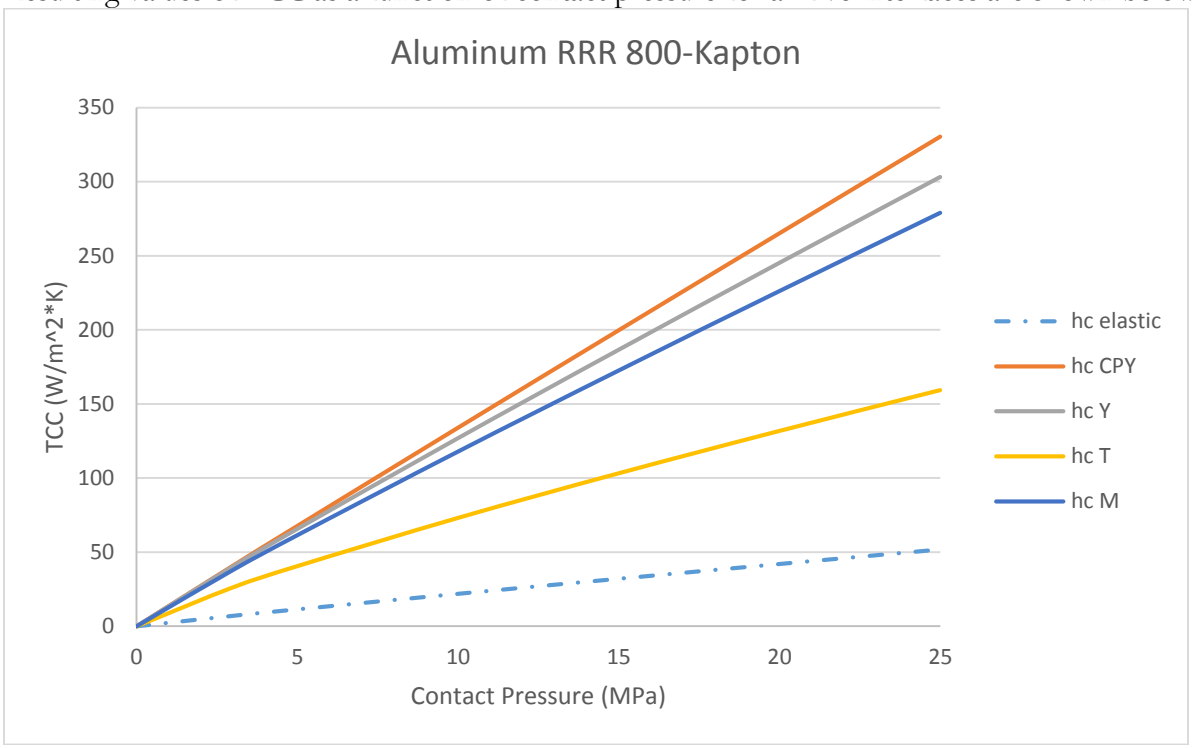

FIGURE 10. TCC VS CONTACT PRESSURE FOR ALUMINUM RRR 800-KAPTON JOINT

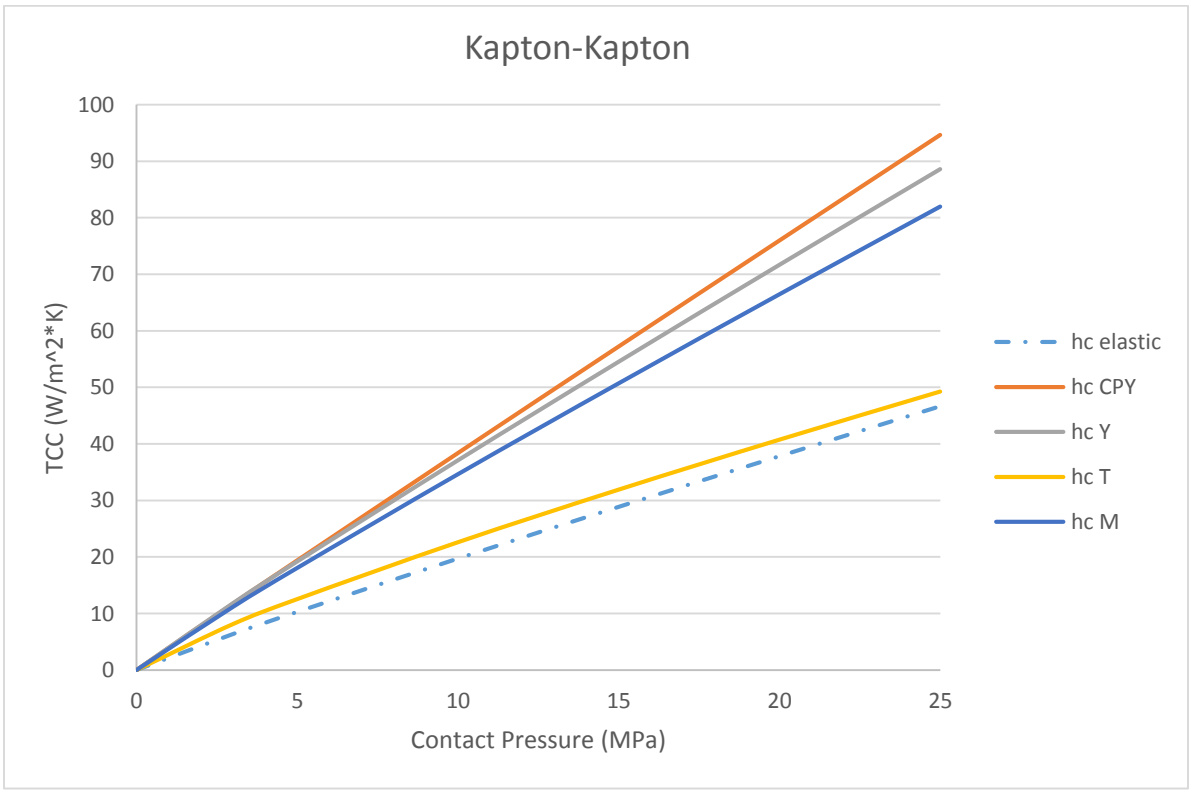

FIGURE 11. TCC VS CONTACT PRESSURE FOR KAPTON-KAPTON JOINT

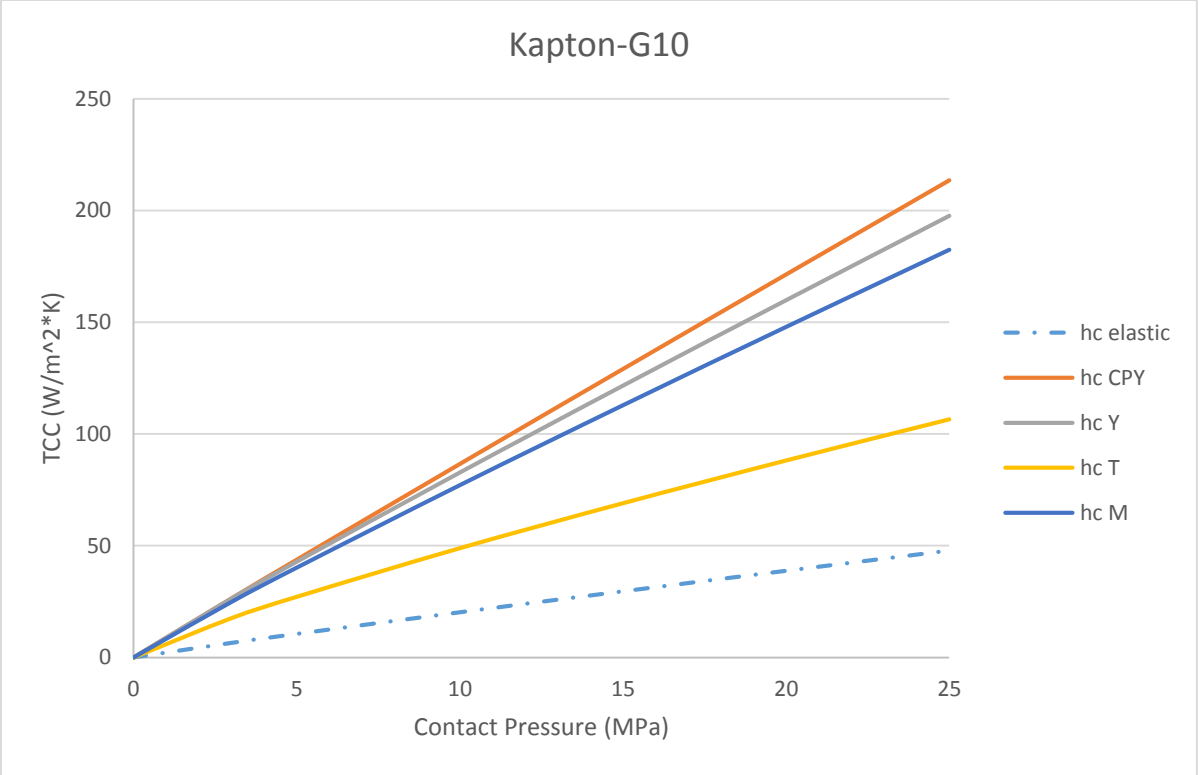

FIGURE 12. TCC VS CONTACT PRESSURE FOR KAPTON-G10 JOINT

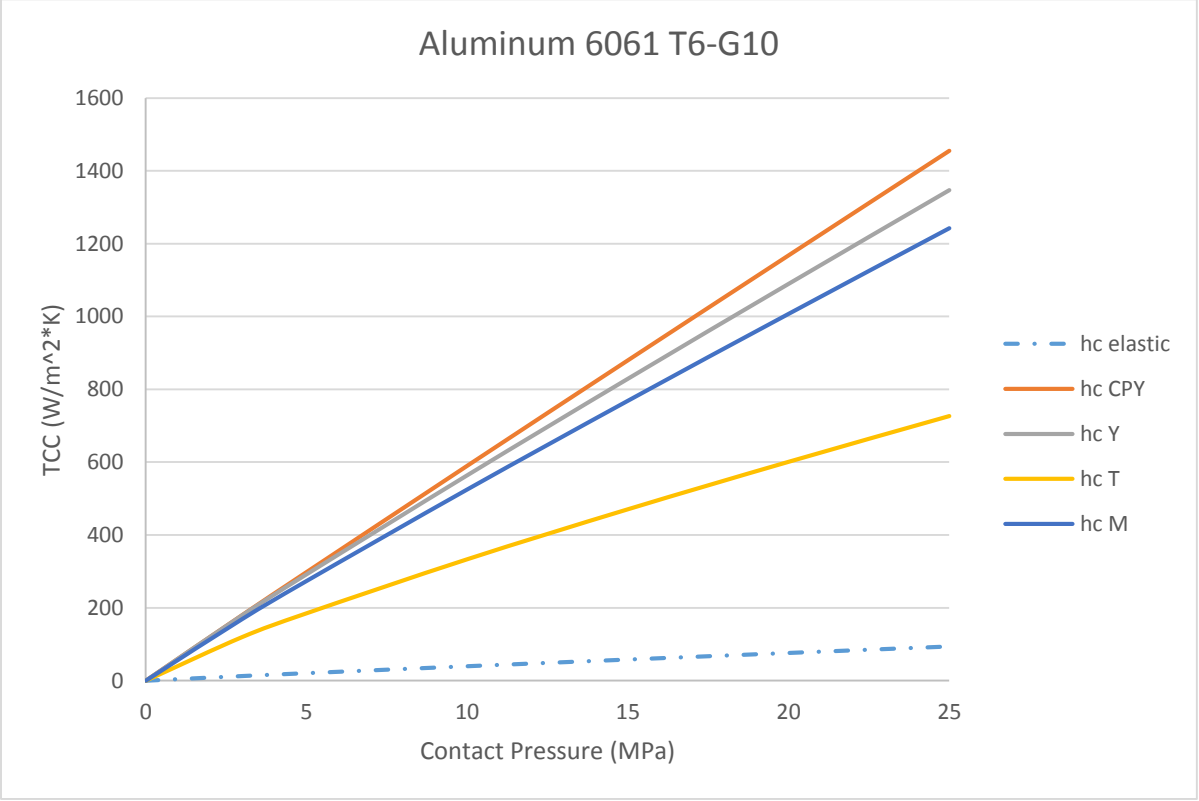

FIGURE 13. TCC VS CONTACT PRESSURE FOR ALUMINUM 6061 T6-G10 JOINT

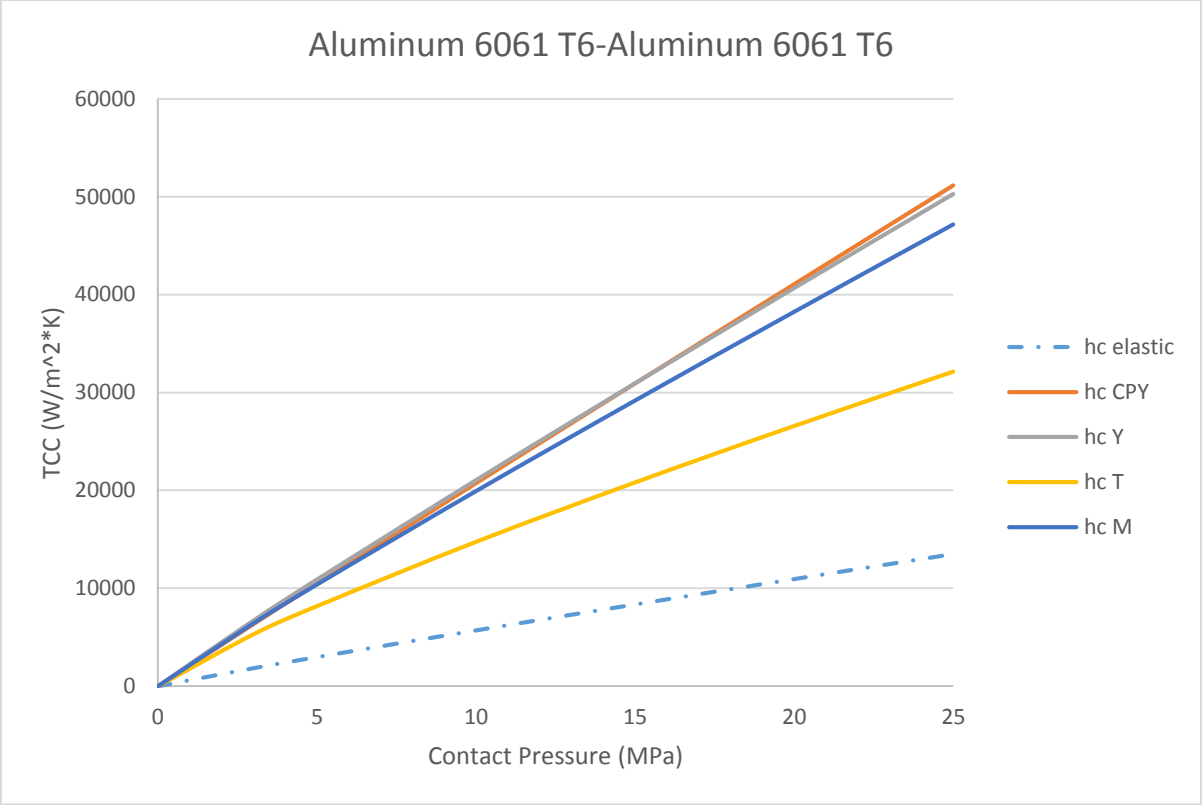

FIGURE 14. TCC VS CONTACT PRESSURE FOR ALUMINUM 6061 T6-ALUMINUM 6061 T6 JOINT

As we expected, Tien's model is the most conservative among plastic models.
Elastic model gives much lower values for TCC if compared to plastic models. The reason for this is that the contact area in pure plastic deformation is larger than in elastic deformation (according to Mikic model, the ratio is two).

4. Simulation results

Bolts generate an uneven contact pressure distribution. Real contact pressure distribution have to be determined to perform a more realistic steady-static thermal analysis.

4.1. Static Structural Analysis

The results of a static structural analysis performed on the clamped surface of the superconductor are shown in figure 15, 16, 17. They show the real contact pressure distribution on the superconductor in three significant cases: 3.559 KN (800 lb) preload and 1 mm G10 insulator, 6.005 KN (1350 lb) preload with 1 mm G10 insulator, 6.005 KN (1350 lb) preload with 0.5 mm G10 insulator.

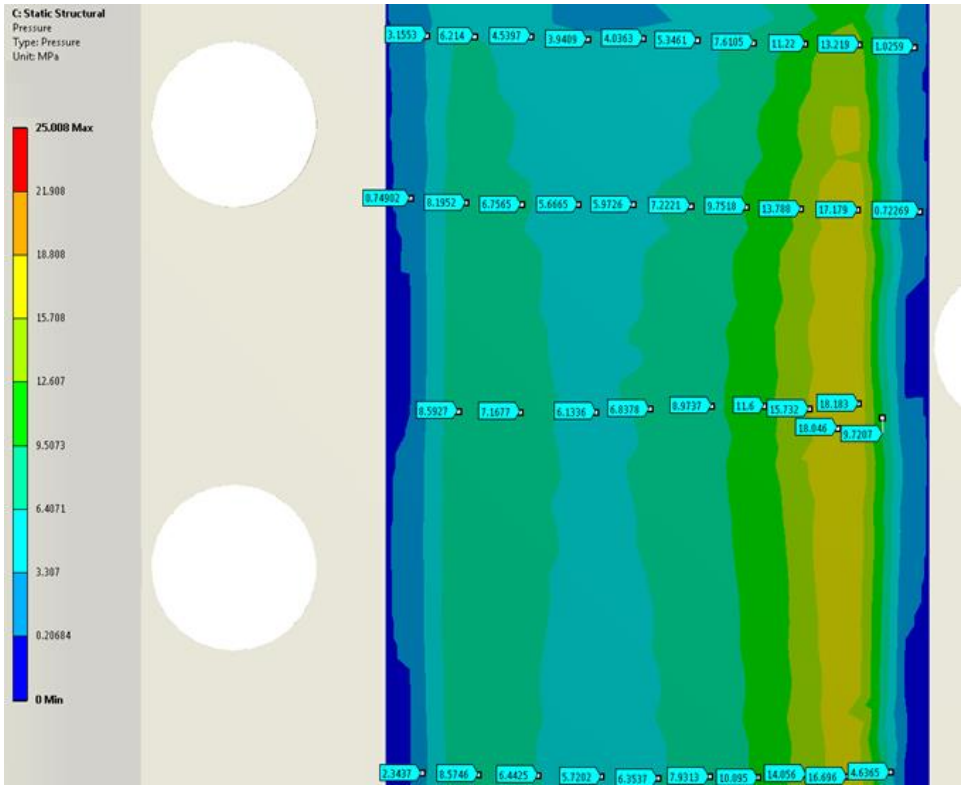

FIGURE 15. STATIC STRUCTURAL ANALYSIS WITH 3.559 KN (800 LB) BOLT PRELOAD, 1 MM G10 INSULATOR (IMAGE COURTESY OF VALERI POLOUBOTKO)

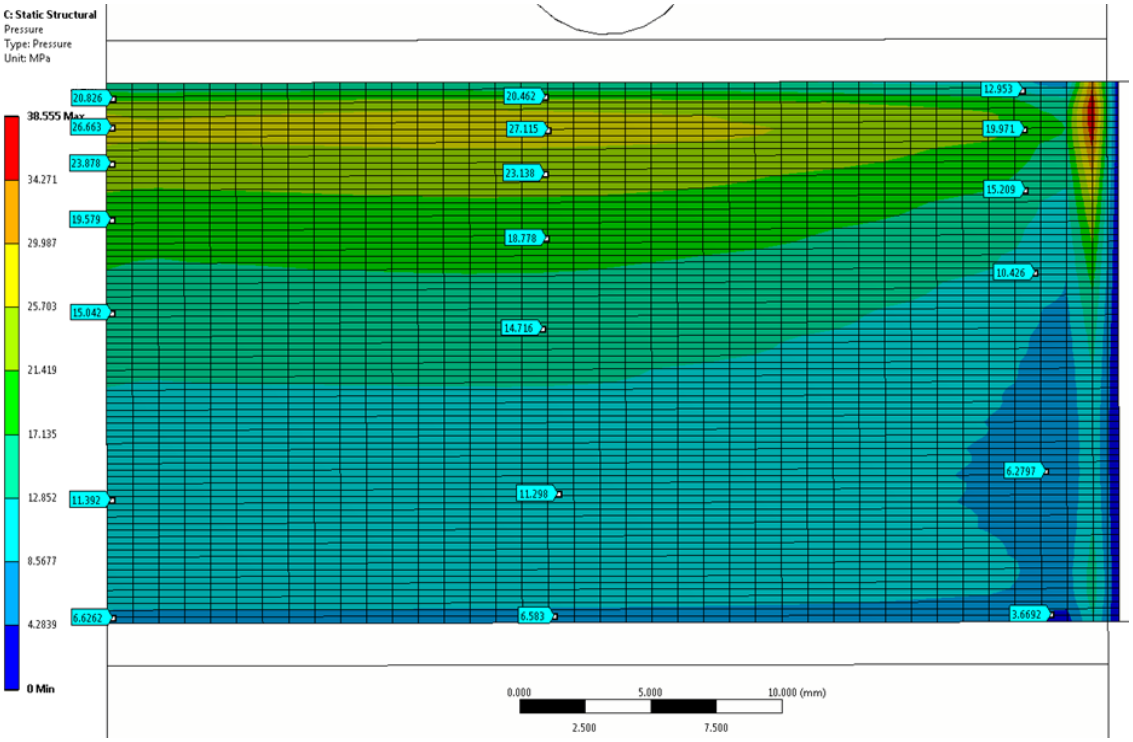

FIGURE 16. STATIC STRUCTURAL ANALYSIS WITH 6.005 KN (1350LB) BOLT PRELOAD, FRICTIONLESS, 0.5 MM G10 INSULATOR (IMAGE COURTESY OF VALERI POLOUBOTKO)

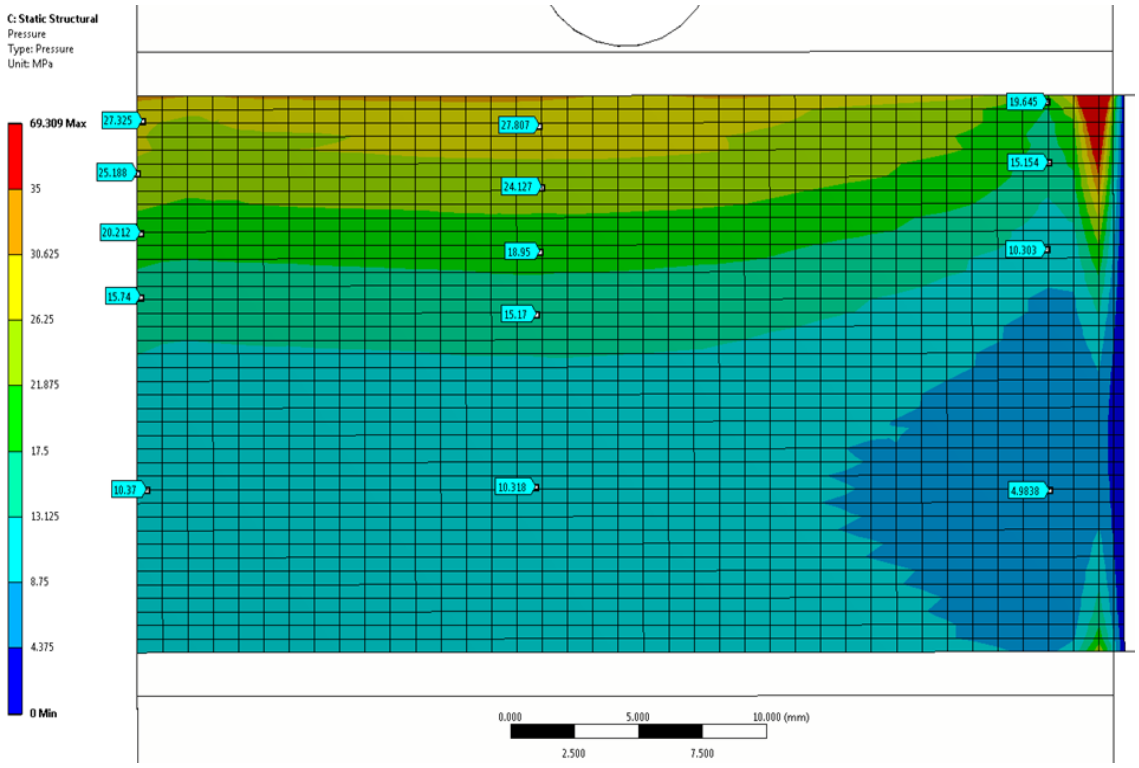

FIGURE 17. STATIC STRUCTURAL ANALYSIS WITH 6.005 KN (1350LB) BOLT PRELOAD, FRICTIONLESS, 1 MM G10 INSULATOR (IMAGE COURTESY OF VALERI POLOUBOTKO)

Analyzing static structural analysis results, the clamped surface was divided into four main zones with similar values of contact pressure. In each zone an average pressure was applied in Ansys thermal simulations.

4.2. Steady-Static Thermal Analysis

The values of thermal contact conductance for all five interfaces have been calculated for real average contact pressures on clamp contact surface and a steady-state thermal analysis have been performed for the three cases reported above.

As far as the 3.559 KN preload case is concerned, maximum temperatures reached in the superconductor are too high (10.8 K in elastic model, 7.5 K in plastic model).

For 6.005 KN preload, simulations have been performed for 250 mm and 500 mm of distance between contiguous clamps, for two thicknesses of G10 insulator (1 mm and 0.5 mm) for both plastic and elastic models. Results are reported in Table 3.

TABLE 3. MAXIMUM TEMPERATURES IN THE SUPERCONDUCTOR FOR 250 MM AND 500 MM OF DISTANCE BETWEEN THE CLAMP, 0.5 MM AND 1 MM G10 INSULATOR FOR BOTH PLASTIC AND ELASTIC MODELS

		0.5 mm G10		1 mm G10	
		T_{max} (K)	T_{max} in superconductor (K)	T_{max} (K)	T_{max} in superconductor (K)
250 mm	elastic	5.96	5.84	6.06	5.94
	plastic	5.47	5.35	5.56	5.43
500 mm	elastic	7.64	7.51	7.89	7.77
	plastic	6.41	6.29	6.63	6.51

Temperature results show that 500 mm of distance between the clamps is definitely too long to cool the conductor properly down. On the other hand, there are not significative temperature differences between 0.5 and 1 mm G10 insulator. 1 mm G10 (the dimension originally suggested by magnet designers) is already enough to keep the superconductor below 6 K. A thicker layer of G10 could also ensure better protection of kapton from the direct contact of the clamp (kapton can easily tear, especially in presence of impurities).

Some pictures of temperature distributions are reported below.

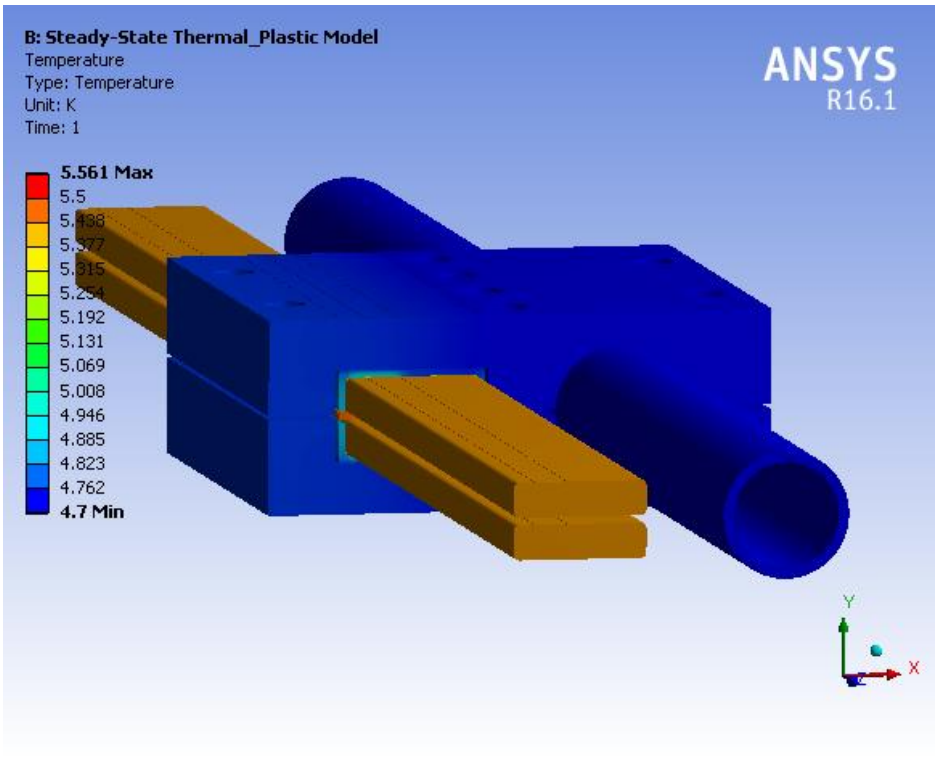

FIGURE 18. TEMPERATURE DISTRIBUTION ACROSS THE ASSEMBLY, 1 MM G10 INSULATOR, 250 MM CONDUCTOR LENGTH, PLASTIC MODEL

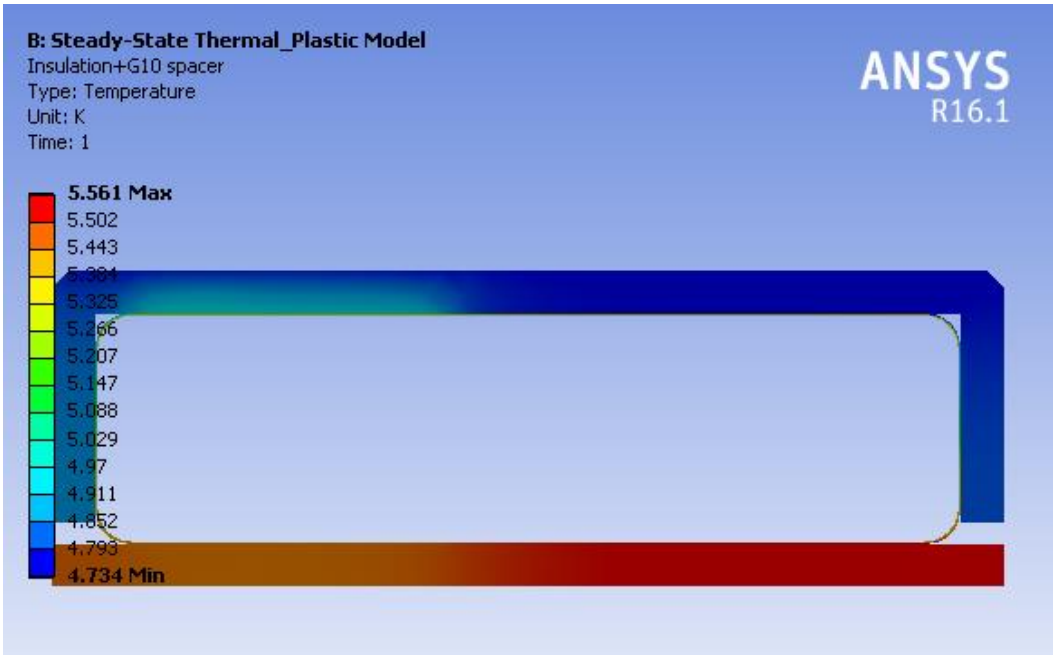

FIGURE 19. TEMPERATURE DISTRIBUTION ACROSS INSULATION, 1 MM G10 INSULATOR, 250 MM CONDUCTOR LENGTH, PLASTIC MODEL

The maximum temperatures are reached in the G10 spacer, which is the only electrical insulator between the conductors although it doesn't play any thermal role. The uneven pressure distribution is reflected on temperature distribution: the zones with higher contact pressure have higher thermal contact conductance in joints, which allows a high heat flux, as shown in figure 19. On the contrary, in zones with lower contact pressure heat flux is prevented (see right part of figure 19).

As we expected, temperature difference along Niobium Titanium superconductor are negligible (2 mK), which implies that there are no parts at risk of quench more than others.

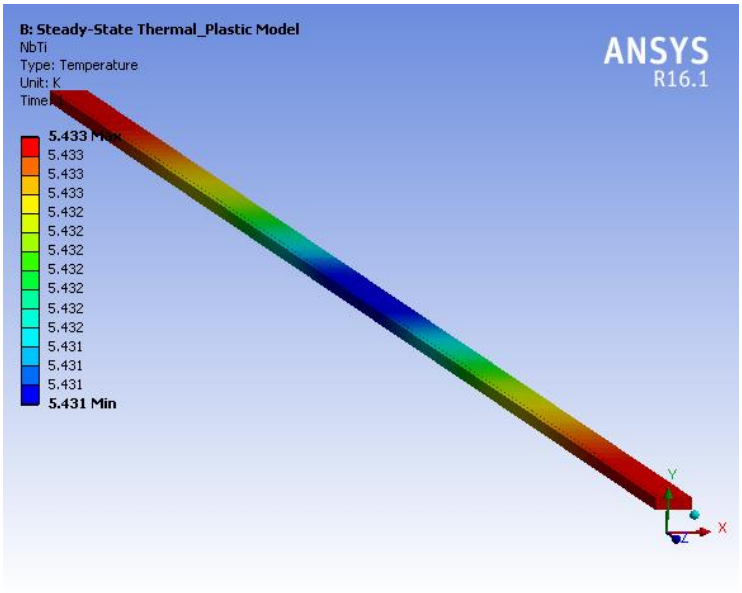

FIGURE 20. TEMPERATURE DISTRIBUTION ALONG NBTI, 1 MM G10, INSULATOR, 250 MM CONDUCTOR LENGTH, PLASTIC MODEL

5. Clamp test

5.1. Test Components

- Cernox RTD
- Sylicon Diodes #Si410A read out by a Scientific Instrument (Model 9308)
- 3x35 Ohm kapton film heaters (Minco model #HK5578R350L12A)
- LakeShore readout (Lakeshore Model #340)
- Detector Solenoid sample conductors
- Two voltage and current DMMs (HP model 3457A)
- Cryocooler (Cryomech model #PT415, Helium Compressor Model)
  Cooling capacity: 40 W at 45K (first stage)
  1.5 W at 4.2K (second stage)
  Base temperature: 2.8K with no load

5.2. Measurements

The "two-heater method" by Didschuns [4] is used for all the testing. With this technique, a heater is mounted on the "cold end" (the pipe) and one heater and a sensor are mounted on the "hot end" (the superconductor). There are practical and economic advantages in applying this: first of all, heat can be easily applied and accurately controlled to the ends (cold end and hot end); moreover, the use of just one sensor reduces calibration error than if we used multiple sensors besides reducing the total cost of the setup. Keeping the cold end temperature constant both simplifies the analysis and reproduces real situation where liquid helium is at the fairly constant temperature of 4.7 K.
To take the data, the test silicon diode temperature on the superconductor is measured for different applied heat loads. In order to maintain the cold end temperature constant, the power of the control heater is adjusted.
The experiment is conducted as follows:

- The hot end heater is powered with a known heat flux (Q) and the steady-state hot end temperature recorded;
- hot end heater is switched off and cold end one is powered with the same heat flux (Q); hot end steady-state temperature is recorded.

During measurements, copper shield temperature, cold head temperature and control temperature are monitored to check that they remain constant.

Two silicon diodes are put on hot end, one on each sample conductor, to check if the temperature distribution is symmetrical.

5.3. Test setup

Test setup scheme is represented in figure 22.

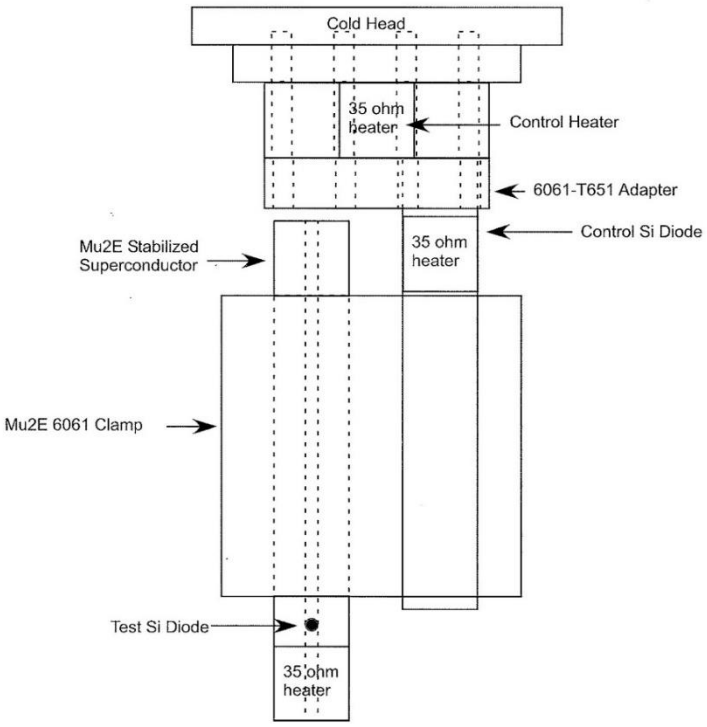

FIGURE 22. TEST SETUP SCHEME

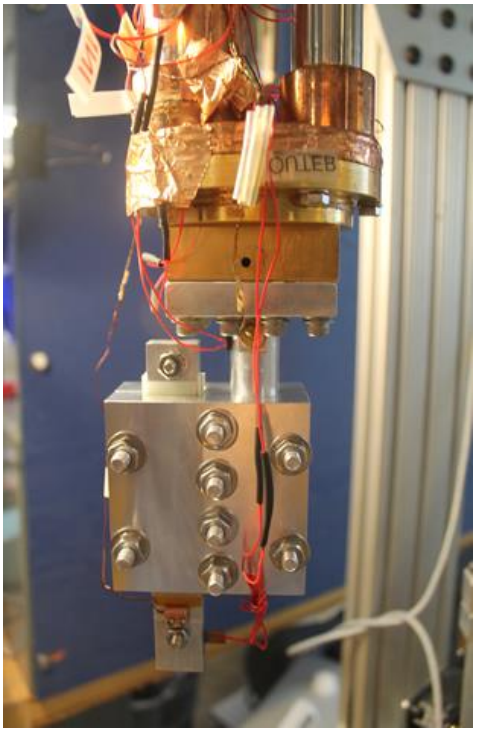

FIGURE 21. CLAMP ASSEMBLY

The aluminum plate connected to the pipe is bolted to an aluminum 6061-T651 adapter bolted to a golden plate connected to the cold head (figures 21 and 22).
The whole assembly is inserted into a copper shield (figure 23). A silicon diode is mounted on the shield to check that its temperature is constant (22.7 K). The copper shield is wrapped into Multilayer Insulation (MLI, figures 23 and 24) and inserted into the cryostat (figure 24).

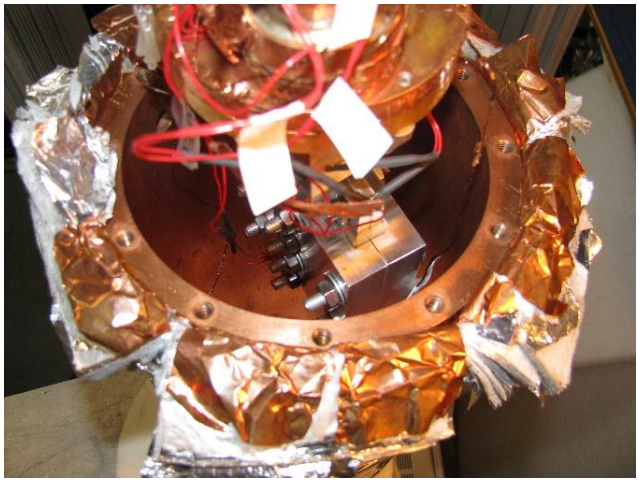

FIGURE 23. COPPER SHIELD AND MLI

FIGURE 24. CRYOSTAT

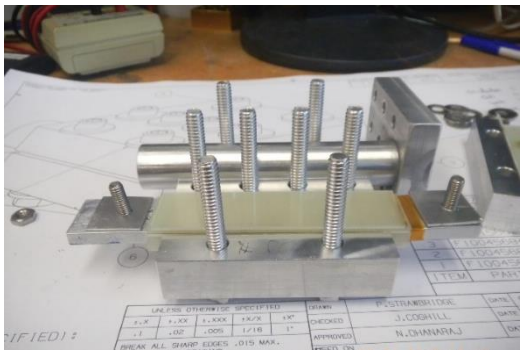

FIGURE 26. G10 SPACER

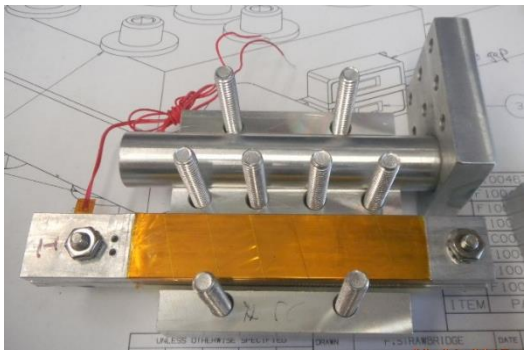

FIGURE 25. SUPERCONDUCTOR WRAPPED IN KAPTON LAYERS

The insulation scheme consists of 1 mm G10 insulator and two layers of kapton 25.4 μm each. G10 spacer originally was 1.5 mm thick but issues during the assembly induced to machine the spacer again and eventually introduce one more spacer.

Dimensions of the components can be found in Appendix 1, except for the later modifications which will be available in the future.

Bolts are Aluminum 2024-T4, with nominal diameter 6.4 mm (0.25"). The torque is gradually increased until 9 N-m (80 in-lb), which corresponds to a clamping force of 2.33 KN (524 lb), much less than the contact pressure applied in Ansys simulations.

5.4. First set of Results

Since we had problems during the assembly, we were able to perform just one test. The first set of results is shown in Table 4.

TABLE 4. RESULTS FOR THE FIRST COLD TEST

Conductor1 Temp. (K)	Conductor2 Temp. (K)	Control Temp. (K)	Cold Head Temp. (K)	Shield Temp. (K)	Power (W)	Notes
6.559	7.731	4.540	4.9	22.662		Setpoint to 4.7K
6.676	7.835	4.702	5.0	22.699	0.01	Inner heater on
6.685	7.843	4.702	4.9	22.742	0.01	Inner heater off
					0.012	Outer heater on
6.872	8.036	4.700	4.9	22.750	0.012	Outer heater off
					0.021	Inner heater on
6.691	7.847	4.700	4.9	22.738	0.021	Inner heater off
					0.020	Outer heater on
7.008	8.175	4.700	4.9	22.733	0.020	Outer heater off

					0.032	Inner heater on
6.705	7.859	4.700	4.9	22.622	0.032	Inner heater off
					0.032	Outer heater on
7.190	8.361	4.700	4.9	22.605	0.032	Outer heater off
					0.041	Inner heater on
6.701	7.852	4.700	4.9	22.622	0.041	Inner heater off
		4.790			0.041	Outer heater on
7.556	8.728	4.790	4.9	22.609	0.041	Outer heater off
					0.051	Inner heater on
6.794	7.937	4.850	4.9	22.619	0.051	Inner heater off
		4.860	4.9		0.051	Outer heater on
7.797	8.965	4.860	4.9	22.628	0.051	Outer heater off

First cold test was not successful. Setting the cold head setpoint at 4.7 K we would expect a lower temperature in the superconductors. Moreover, temperature doesn't distribute symmetrically, there are significant temperature differences between the two superconductors. The reason may be that the contact between surfaces is not perfect, it' necessary to check the assembly and apply a higher clamping force. A clamping force of 2.334 KN was applied (which corresponds to a contact pressure of 7 MPa), much lower than the one applied in the simulations (6.005 KN). A lower clamping force implies higher thermal contact resistance which causes a higher drop of temperature across joints.

Yield stress tests on 2024 aluminum bolts have shown that after 2.624-2.920 KN bolts may yield. Therefore, to increase the torque and consequently allow a better heat transfer through the joints high strength bolts (for instance, 7075 aluminum bolts) are required.

5.5. Estimated Results

The heat load corresponding to 0.2 W/m is 0.02 W (results for this heat load are in red ink in Table 4). Interpolating the results of the simulations for a preload of 3.559 and 6.005 KN we obtain the expected temperature for the superconductor for 2.335 KN preload (preload applied in the test). Interpolation is reported in picture 27.

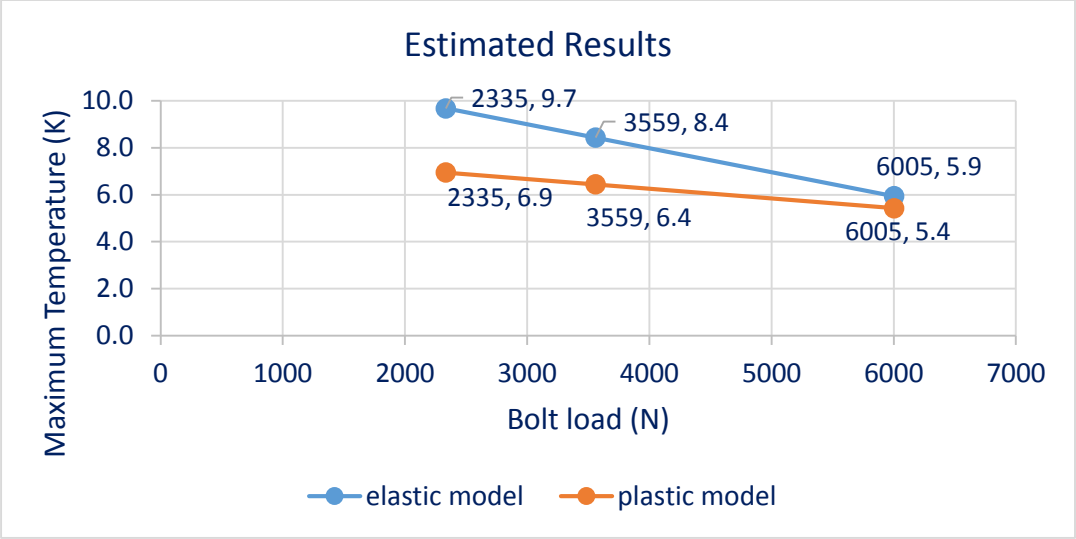

FIGURE 27. ESTIMATED RESULTS FOR 2.335 KN (TEST PRELOAD)

Expected temperature is around 6.9 K (plastic model) and surely lower than 9.7 (elastic model). The experimental data for temperature of the two superconductors from the first test range between 6.7 and 8.2 K. It's thus reasonable to evaluate our simulations and our TCC models quite realistic even if other tests are necessary to definitely verify the model.

6. Summary and next steps

In this report the design, stress and thermal analysis and test of transfer line clamps have been illustrated. After designing the clamp with NX CAD, insulation scheme has been optimized performing both stress analysis and steady-state thermal analysis using the commercial software Ansys. As main results of the simulations, we set the distance between two contiguous clamps at 250 mm and we verified that a 1 mm G10 insulator is sufficiently thin to allow a proper cool down of the NbTi superconductor, thickness which also respects the electrical requirements calculated by magnet designers and assures a good protection of kapton. Secondly, simulations shows that to maintain the temperature below 6 K a preload of 3.559 KN (800 lb) is not sufficient, at least 6.005 KN (1350 lb) of preload is needed.

The clamp has been manufactured and the test performed once. Unfortunately we have run into some issues maybe due to imperfect contact between some parts in addition to very low contact pressure applied (2.33 KN=524 lb), imposed by the bolts used which yield at 2.624-2.920 KN (590-656 lb) preload. Interpolating simulation results we calculated expected temperature in the superconductor for 2.334 KN: experimental data fall in the range between plastic and elastic model which make our simulations quite realistic or at least conservative, since a higher contact pressure or a better contact between the clamp and the superconductor would facilitate the cool down.

As far as next steps are concerned, after checking the assembly, a new cold test should be performed with high strength bolts to apply a higher clamping force (around 6 KN according to our simulations).

References

[1] B. B. Mikic, *Thermal Contact Conductance; Theoretical Considerations*, International Journal of heat and mass transfer, pp. 205-214

[2] M. M. Yovanovich, J. R. Culham and P. Teertstra, *Calculating Interface Resistance*, http://www.mhtlab.uwaterloo.ca/pdf_papers/mhtl97-4.pdf

[3] V.W. Antonetti, T.D. Whittle, and R.E. Simons, *An Approximate Thermal Contact Conductance Correlation*, HTD-Vol. 170, Experimental/Numerical Heat Transfer in Combustion and Phase Change, 1991, pp. 35-42

[4] I. Didschuns, A.L. Woodcraft , D. Bintley, P.C. Hargrave, *Thermal conductance measurements of bolted copper to copper joints at sub-Kelvin temperatures,* Cryogenics 44 (2004), pp. 293-299

[5] R.L. Schmitt, G. Tatkowski, M. Ruschman, S. Golwala, N. Kellaris, M. Daal, J. Hall, E.W. Hoppe *Thermal conductance measurements of bolted copper joints for SuperCDMS,* Cryogenics 70 (2015), 41-46

[6] M. Lambert, L. Fletcher, *Thermal contact conductance of spherical rough metals*, ASME Journal of Heat Transfer 119 (4) (1997) pp.684-690

[7] L. Tanner, M. Fahoum, *A study of the surface parameters of ground and lapped metal surfaces using specular and di_use reection of laser light*, Wear 36 (1976) pp.299-316